ISSN 2349-0292
Impact Factor 3.802

GLOBAL JOURNAL OF ADVANCED ENGINEERING TECHNOLOGIES AND SCIENCES

HYDROCRACKING OF OLEIC ACID USING MODIFIED NIW/SZ-MCM-41 TO PRODUCE ECO-FRIENDLY GREEN FUELS

Ahmed M. Alsabagh, Sarah S.Selim, M. S. Elmelawy, M. A. Ebiad, Aly A. ALY, M. S. Behalob and Salwa A. Ghoneim*

[*] Egyptian Petroleum Research Institute, Nasr City, Cairo, Egypt
Chemistry Department, Faculty of Science, Benha University, Egypt

DOI: 10.5281/zenodo.1250338

ABSTRACT

Oleic acid hydrocracking reactions have been investigated in a batch reactor over sulfide NiW/SZ-MCM-41 catalyst which was synthesized via the wet co-impregnation method. The catalyst was investigated by different instrumental techniques such as XRD, Textural surface properties, FE-SEM, HR-TEM, FT-IR and thermal analysis (TGA-DSC) techniques. Operating conditions of the hydrocracking reaction are; temperature= 425°C, pressure= 4 MPa, reaction Time = 2h, and catalyst weight%=5%. Quantitative gas chromatography detected n-paraffins and iso-paraffins ranging between C5–C18+ included C5-C8 gasoline range, C9-C14 kerosene range and C15-C18 diesel range. The product distribution of the organic liquid product contains 28.57% gasoline range (C5-C8), 53.88% kerosene range (C9-C14) and 16.83% diesel range (C15-C18). Distillation of OLP produced three distillates, gasoline (45-160ºC), kerosene (160-275ºC) and diesel (275-310ºC). The produced kerosene range has good properties compared with the properties of conventional kerosene. These properties made it qualified to use as a source of jet fuel production. Properties of the diesel range distillate obtained were favorable with the UOP –Hydro refining green diesel.

The sulfided NiW/SZ-MCM-41catalyst is viewed as an interesting catalyst for the hydrocracking of fatty acid molecules into gasoline, kerosene, and diesel-range used as green fuel.

KEYWORDS: Green fuels; Hydrocracking; MCM-41; transition metals; Sulfated zirconia; Oleic acid.

INTRODUCTION

Diminishing greenhouse gas emission, decreasing fossil fuel reserves, and expanding world energy demand have induced great interest in transportation fuels from bio-renewable resources. Heterogeneous catalysis is ready to assume a basic innovative part for green fuels and bio refining [1, 2]. There is a need to make alternative energy fuels which must be economically competitive, really feasible and environmentally more adequate. One possible alternative is the fuel delivered from renewable resources for example, vegetable oils. Hydrocracking of vegetable oil engenders high quality renewable diesel which can supplant diesel in vehicles with no significant changes of the motors, while aviation fuel produced from vegetable oils can either directly or as a mix with fossil fuel, be utilized for aviation purposes [3-6]. Hydrotreating has the ability to produce long chain alkanes among others; these long chain alkanes easily fit into the diesel range class and are obtainable at elevated temperatures and pressure in the presence of hydrogen. Cracking will yield shorter chain hydrocarbons to fit the gasoline-diesel range class requiring elevated temperature at normal pressure without the need for hydrogen [7]. A superior approach to produce green fuel is to hydrocrack triglycerides to produce petroleum- like fuels. Biodiesel delivered from hydrocracking is hydrocarbon-like and requires no adjustment in the current motors and additionally has a higher cetane number (about 110) than ordinary diesel fuel (51–60). This process may be accompanied with hydrodeoxygenation (HDO), decarbonylation (DCO), decarboxylation (DCO2), hydrocracking and isomerization or a combination of two or more for transformation of fatty acids in triglycerides into normal and/or iso-hydrocarbons [8-10]. Mesoporous molecular sieves like MCM-41, and SBA-15 with large particular surface area have pulled in significant attraction as catalyst support [11, 12]. MCM-41 is broadly used as catalyst support and hydrogenation catalyst because of its homogeneous hexagonal pore arrays with pore diameters extended from 2 to 10 nm and high specific surface area reaches 1000 m2/g [13]. For this situation, extensive pore size and high surface area of MCM-41 promote catalyst particles to disperse on it, and greater effective mass transfer become found out in the porous structure [14, 15]. MCM-41 was accounted for as a selective catalyst for the cracking of light petroleum distillate [16]. The acidity of MCM-41 can be improved upon surface change, through the addition of strong acid species like sulfate ions [17], sulfated zirconia [18] or heteropoly acids with Keggin-type structures

[19, 20], one or the other on the surface or inside the internal channels of MCM-41. Alteration of MCM-41 by transition metals has been observed to be a practical methodology in making catalytic active sites and improving sites for active metals in the plan of recent catalysts [21].

The main object of this work is to prepare and characterize the sulfided NiW/SZ-MCM-41 catalyst to hydrocrack the fatty acid molecules in order to produce green fuels.

EXPERIMENTAL

Materials

Tetra ethyl ortho silicate, TEOS (98%, Aldrich) and cetyltrimethyl ammonium bromide, CTAB (98%, Aldrich), deionized water, ethanol (99.8%) and zirconyl chloride (99% Sigma–Aldrich), ammonia (28–30%, Sigma–Aldrich), sulfuric acid (97–99 % Sigma–Aldrich). Ammonium meta tungstate hydrate $(NH_4)_6H_2W_{12}O_{40}$. xH_2O (sigma Aldrich 99.99 %) and nickel nitrate hexahydrate (Ni $(NO_3)_2{\cdot}6H_2O$), 99.99% sigma- Aldrich), oleic acid 90% Aldrich.

Catalyst preparation

Preparation of MCM-41:

MCM-41 silica-based mesoporous material was prepared according to the following procedure [22]. A given amount of CTAB was added to deionized H_2O with stirring. After the mixture became clear, ethyl alcohol and liquid ammonia were added to the system, then, TEOS was poured into the mixture directly with stirring. Stirring was maintained for 3h at room temperature. The solid product was recovered by filtration and dried at room temperature for 12h. CTAB was eliminated from the product by calcination at 540°C for 9h.

Preparation of nano-structured sulfated zirconia

Zirconyl chloride was dissolved in deionized water; Liquid ammonia (28–30%) was added drop by drop to the mixture under severe stirring until pH reached 10.0. The solution was refluxed then the sample was treated by 0.5M H_2SO_4 solution at room temperature for 10 minutes. More details were mentioned elsewhere [23]. (Sulfur content present in sulfated zirconia =2.61 wt. %).

Preparation of NiW/ (SZ-MCM-41) catalyst

Sulfated zirconia was mechanically mixed with MCM-41 by wt ratio 1: 3. The metal content of NiW was prepared with 10 wt% Ni and 3 wt% W by the wet co-impregnation of aqueous solutions of $(Ni(NO_3)_2{\cdot}6H_2O$, $(NH_4)_6(H_2W_{12}O_{40}){\cdot}xH_2O)$ on the synthesized SZ-MCM-41 support then the resulting solid was dried and calcined at 450°C for 4h [24].

Sulfiding o fNiW/ (SZ-MCM-41) catalyst

The catalyst was Sulfided (activated) before the experiments using a mixture of dimethyl disulfide (DMDS) in isooctane (5%DMDS) then the mixture was gone through the catalyst bed with stream rate of 1.5 ml/ min at 3.0 MP hydrogen pressure and the reaction temperature at 260°C for 2h then raised to 360°C for 4 hours [25]. Researchers have reported that the presence of sulphur compounds is beneficial for the catalytic activity [26]

Catalyst characterization

X-ray diffraction

XRD patterns were registered by Brucker D8 advanced Powder X-ray diffraction with CuK< α > radiation (< λ > = 0.1542 nm), Ni-filter and common area detector. The diffract grams were identified in the 2< Θ > range of 0.5-70° with step size of 0.02 A° and a step time of 0.605.

N_2adsorption–desorption

Surface area and pore structure of the solid materials were characterized from N_2 adsorption studies at -196° C using a NOVA 3200 apparatus, USA. The samples were previously out-gassed under vacuum (10^{-4}Torr) at 300°C for 24 h. Surface areas (S_{BET}) were estimated from the adsorption data.

Field emission scanning electron microscopy (FE-SEM)

FE-SEM (FEI Quanta FEG250) SEG NewZyland was used to determine particle morphology, distribution and to examine fracture surfaces. The SEM comprises of an electron gun generating a supply of electrons at an energy range of 1-40 KeV.

ISSN 2349-0292
Impact Factor 3.802

Electron-lenses reduce the diameter of the electron beam and place a small focused beam on the sample. The electron beam connects with the near-surface region of the sample to a depth of about 1micrometer and creates indications used to form an image.

High resolution transmission electron microscopy (TEM)
High resolution TEM apparatus (JEOL) JEM 2100 Model (Japan) which attached (EDX) Oxford X-Max was used to examine the pore structure of samples. The powdered material was dispersed in ethanol solution and then sonicated for 5min to ensure a well- dispersed solution. This solution was dropped on a TEM carbon grid and dried in vacuum oven at 438 K to eliminate ethanol in TEM carbon surface area determination of solid samples was measured by Nova surface area analyzer.

Fourier transform infrared (FTIR):
In a typical IR spectrum the wave number plotted on the x-pivot, is corresponding to energy; consequently the highest energy vibrations are on the left. The percent transmittance (%T) plotted on the Y-pivot. The Nicolet Is-10 FT-IR spectrometer was employed to define the functional groups in the catalyst and the kind of the bond that attachés the atoms.

Thermal analysis (TGA & DSC):
Simultaneous DSC & TGA equipment or SDT Q600 is analysis equipment able to perform both differential scanning calorimetry (DSC) and thermal gravimetric determination (TGA) Simultaneous. The SDT measures the heat flow and weight changes joined with transitions and reactions in the temperature ranging from 25ºC to 1500ºC. The data gave differentiates exothermic and endothermic events, which have no associated weight change (e.g. melting and crystallization) from those that include a weight change (e.g. degradation).moreover performing DSC & TGA measurements at the same time ,on the same tool and identical pattern ,gives greater productivity and disposes of experimental and examining factors as components inside the investigation of data.

Temperature programmed desorption (TPD)
Temperature programmed desorption of ammonia was measured on a CHEMBET 3000 chemical absorber (Quantachrom) JAPAN, INC. Before evaluations, the samples were activated at 500 °C for 1 h in presence of helium atmosphere. After the temperature cooled to 100 °C, the samples were cleaned by ammonia for 1.5 h and then the gas was converted into helium to get rid of the physically adsorbed ammonia molecules, until the baseline was flat. After this, the temperature was raised to 700 °C with a ramping rate of 10°C /min to attain the NH_3–TPD

Oleic acid hydrocracking experiments
The hydrocracking experiments were operated in a high pressure batch autoclave (Parr model 4575) with an inner volume of 500 ml and heated by a digital controller.

The operating conditions were: temperature 425°C initial hydrogen pressure 4 MPa catalyst wt. % 5 and the reaction period was 2hrs for each run. In a typical run 180 g of the oleic acid sample was placed into the reactor. The system was heated at a rate of 20°C min^{-1} and speed of 500 rpm. The autoclave was shut down then left to cool for 8 hours.

The liquid products (organic and aqueous fractions) were collected in liquid samplers. The aqueous phase and catalyst were separated from liquid products using a syringe then filtration. The organic liquid products (OLP) were then weighed to determine the yield of OLP then stored in glass containers for subsequent analysis. The gaseous products were measured with wet-type gas flow meter then released.

Yield (wt. %) = the organic liquid products (wt.) / Oleic acid feed (wt.) x 100

The OLP was distilled in simple distillation process using Aldrich distillation column (length 20 cm), internal diameter 3cm) and U-shaped glass tube manometer for measuring the pressure. Distillation was carried out under atmospheric pressure for fraction collected up to 160◦C. Vacuum distillate at 50 mmHg was carried out to collect the fractions 160-275◦C and 275-310◦C. The three fractions were subjected to analysis according to ASTM methods.

ISSN 2349-0292
Impact Factor 3.802

GC analysis

OLP was analyzed by gas chromatography (Agilent 7890A) equipped with flame ionization detector (FID), mobile phase (carrier gas) was $N_2$and HP-5 column (length 30 m, internal diameter 0.32 mm, film thickness 0.25 Mm). The following temperature program was used for analysis: 50°C (10 min) by ramp 4°C / min to 300 °C (20 min).

RESULTS and DISCUSSION

Characterization results

Low angle X-ray diffraction

XRD diagram of MCM-41 in Fig.1(a) exhibited intense peak at 2.43 degree due to (100) plane reflection lines and this illustrated the forming of organized mesoporous materials and this peak are recorded in agreement to the hexagonal regularity of MCM-41 in general. On the other hand, Fig.1(b) For nano-structured sulfated zirconia gave diffraction peak at 2Θ =2.22 in the low angle area illustrating the porosity of nano-sulfated zirconia with regular pore in short range [27]. Fig.1(c) for NiW/SZ-MCM-41 composite showed 2Θ at 2.1 indicated that, incorporation of SZ and NiW resulted in partial destruction of hexagonal ordering in mesoporous MCM-41 as can be shown from the decreasing in peak intensity.

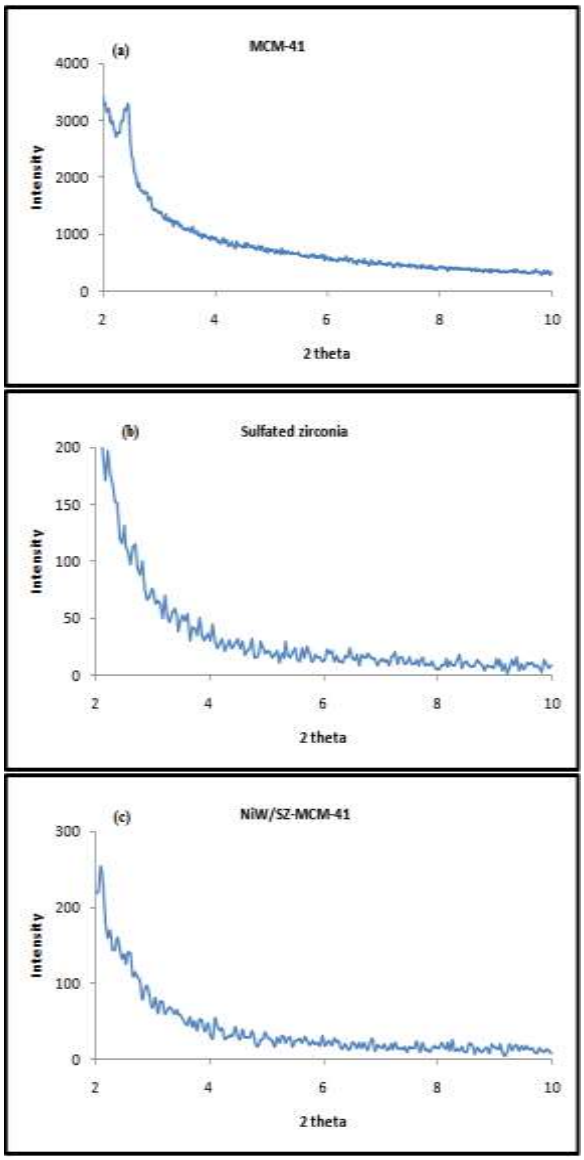

Fig. 1: XRD of the current catalysts

N_2 adsorption–desorption:

Nitrogen physisorption isotherms of the MCM-41, nanostructured sulfated zirconia and NiW/SZ-MCM-41 samples are utilized to get data about the porosity and textural properties. The relating textural properties are abbreviated in the nitrogen physisorption isotherms are described by atypical IUPAC sort IV which is particular for mesoporous materials. Fig. 2(a) indicated that, the Pure MCM-41 illustrated clear H1 type hysteresis loop in the relative pressure range between 0.22 and 0.35, implying presence of very regular mesoporous channels with BET surface area equal to 1448.66 m^2/g and total pore volume is 0.87 cc/g. Fig 2(b) illustrated BET surface area equal 62.08 m^2/g and its pore size distribution proved that sulfated zirconia in nanoscale and this confirmed by its XRD. Fig. 2(c) for NiW/SZ-MCM-41composite indicated a slight shift of p/p° (0.44-0.92) which proved that the composite found in micro and mesostructure and acquired BET of444.48 m^2/g and total pore volume was 0.30 cc/g. the following Table showed the physical properties of the current catalysts:

Table (1) physical properties of the current catalysts

catalysts	**S_{BET} (m^2/g)**	**V_P (cc/g)**	**D_p (nm)**
MCM-41	1448.66	0.87	2.4
sulfated zirconia	62.08	0.09	3.81
NiW/SZ-MCM-41	444.48	0.30	2.21

The sudden decline of pore size, volume and surface area is an explanation that major of the loading of sulfated zirconia and NiW are inside the pores. In order to maintain the porous structure in the NiW/sulfated zirconia-MCM-41 middle content of sulfated zirconia (20-25%) was used. N_2 adsorption desorption isotherms of MCM-41 and NiW/ sulfated zirconia -MCM-41 in Fig.2(a) and (c) are very much alike in shape and the two are type IV curves. This indicated that, the regularity of the hexagonal arrays of the mesoporous MCM-41 was not much influenced where as the capillary condensation step moved slightly towards the lower partial pressure, the comparable pore size distribution detected by BJH technique which is illustrated in Fig.2 (a, c) as NiW/SZ-MCM-41 exhibited less pore volume, slightly boarder pore size dispersion and smaller pore radius than pure MCM-41.

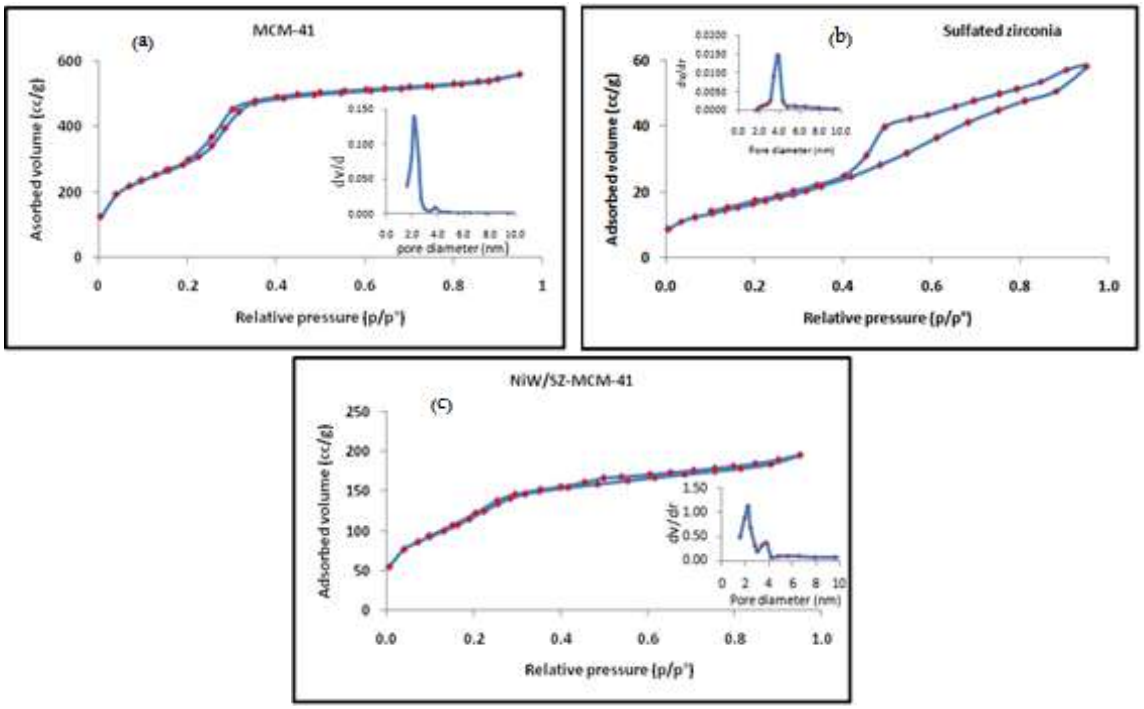

Fig.2:N_2 adsorption-desorption isotherms and pore size dispersion for the current catalysts: a) MCM-41; b) Sulfated zirconia and c) NiW/SZ-MCM-41.

ISSN 2349-0292
Impact Factor 3.802

Field Emission Scanning Electron Microscopy (FE-SEM)

FE-SEM of synthesized mesoporous silica MCM-41 illustrated in Fig. 3 images (a), (b) and (c) showed a regular spherical morphology in shape, uniform in size and a clean surface. The SEM of sulfated zirconia shown in Fig 3 images (d), (e) and (f) indicated that ZrO_2 has surface shining after sulfation. This may be due to the presence of highly charged species (SO_2^{-4} ions). The SEM of NiW/SZ-MCM-41 catalyst shown in Fig .3 images (g), (h) and (i) proved that the good impregnation of $SZrO_2$ crystals and Ni W oxides on the surface of spherical MCM-41.

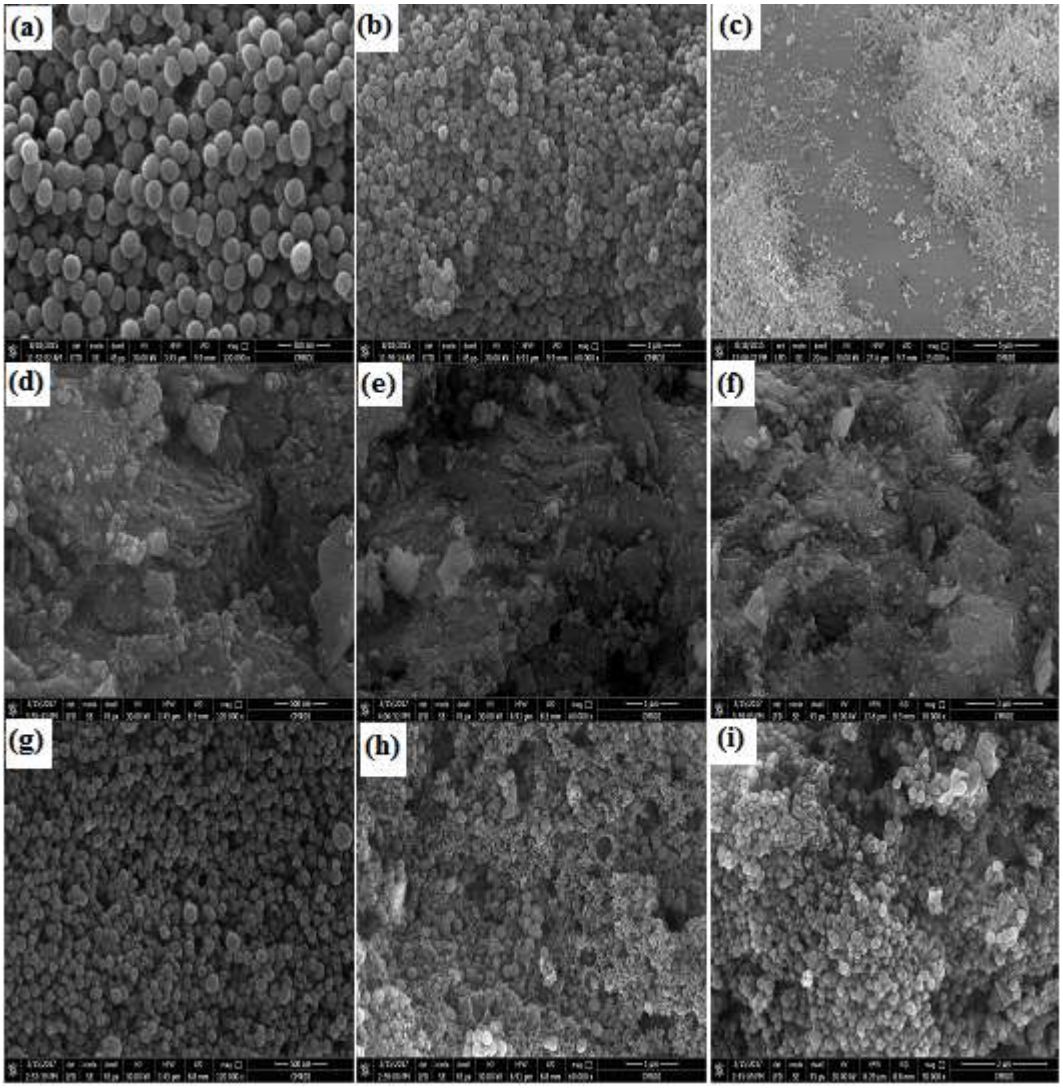

Fig.3: FE-SEM images: (a), (b) and (c) for MCM-41, (d), (e) and (f) for nanostructured sulfated zirconia, (g), (h) and (i) of NiW/SZ-MCM-41 catalyst at lower and higher magnification

High resolution transmission electron microscope (HRTEM) analysis

High resolution transmission electron micrographs viewed in Fig.4 images (a, b and c) showed a regular hexagonal array of uniform channels in a hexagonal arrangement of pure MCM-41, Fig.4 images (d ,e and f) for sulfated zirconia indicated that it has ordered and porous structure and also Fig. 4 images (g, h and i) for NiW/SZ-MCM-41 catalyst showed regular hexagonal array of uniform channels indicated that highly ordered pore structure which means that there was no bulk aggregation inside and outside the pores.

ISSN 2349-0292
Impact Factor 3.802

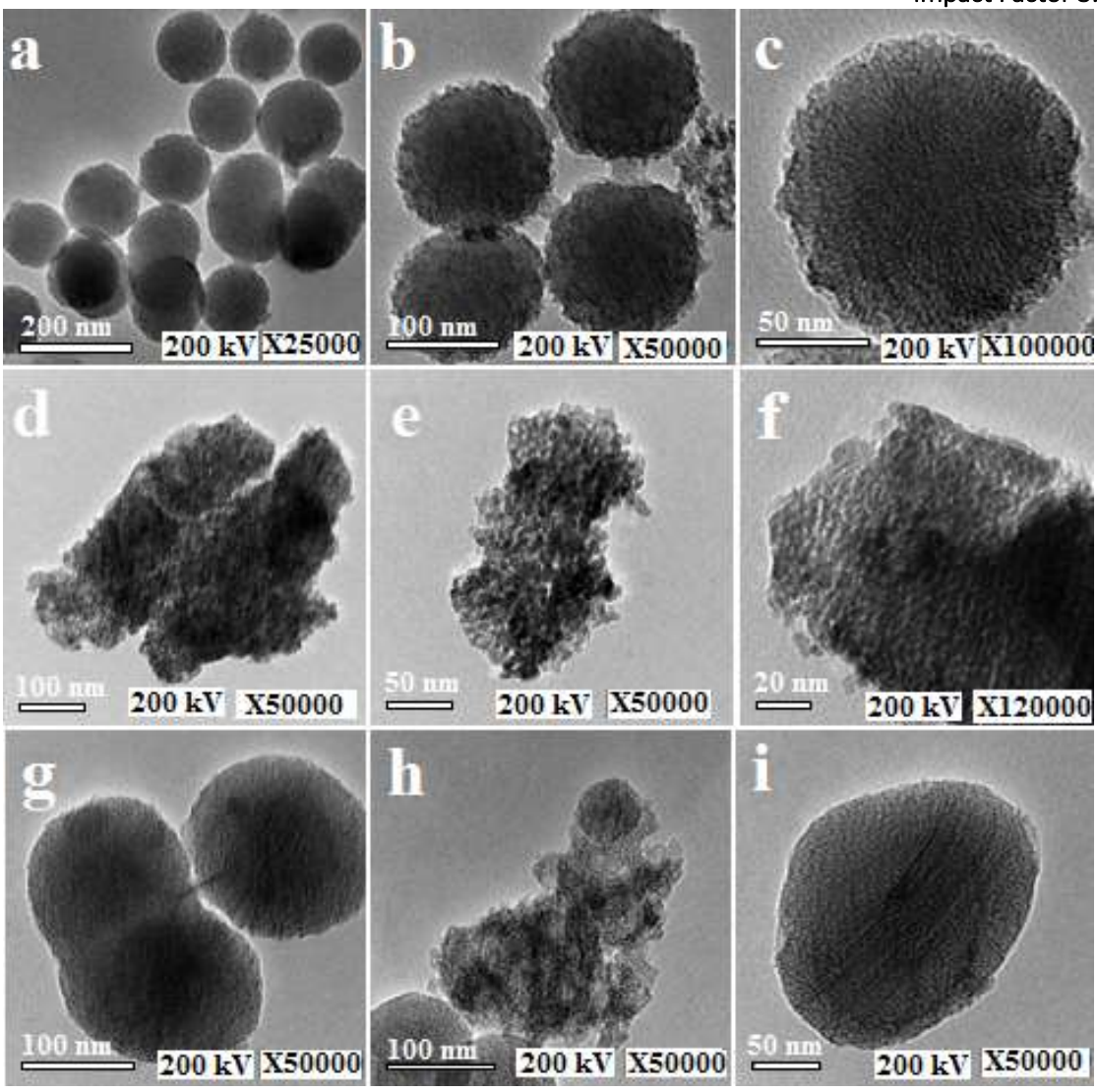

Fig. 4: TEM images:(a), (b) and (c) for MCM-41, (d), (e) and (f) for nanostructured sulfated zirconia, (g),(h) and (i)of NiW/SZ-MCM-41 catalyst at lower and higher magnification.

FT-IR analysis

FT-IR spectrum of unloaded MCM-41 in Fig. 5(a) indicated a broad band at 3429 cm^{-1}, that is due to the hydroxyl groups and silanol groups on the external and internal structure. A band at 1629 cm^{-1} is –OH group, it may be due to water interacting with the support surface. Indeed, bands at 1090 cm^{-1}, 965 cm^{-1} and 808 cm^{-1} are because of symmetric and asymmetric stretching of the Si-O-Si bond, which are very familiar in silicates while adsorption bands at 458 cm^{-1} correspond to the bending vibration of Si-O-Si groups. Fig. 5(b) for the nano-structured sulfated zirconia showed intense and wide band at 3432 cm^{-1} owing to physisorbed and coordinated water which associated with the band at 1633 cm^{-1} due to the bending mode (υHOH) of coordinated water. The band at 1401 determined covalent S==O bond. The bands detected at 1141–967cm^{-1} reference to the asymmetric stretching for the sulfate groups (partially ionized S== O double bonds and S–O single bonds) with zirconia in a chelating bidentate mode. The bands between (744-500) cm^{-1} are characteristic to crystalline zirconia [28]. Fig. 5(c) for NiW/SZ-MCM-41 showed a band at 967cm^{-1} has been attributed to a Si–O–Zr asymmetric stretching [29]. In addition, a peak at 3417 cm^{-1} is because of O-H stretching of water which is associated with O-H bending at 1634 cm^{-1}. The peak at 797 cm^{-1} is attributed to Si-O stretching mode a weak band at 600 cm^{-1} that corresponds to the existence of ZrO_2 in MCM-41. The peak at 465 cm^{-1} indicated the bending vibration of Zr-O-Si groups. The absence of 425 cm^{-1} band indicated that ZrO_2 is highly dispersed in the silica framework.

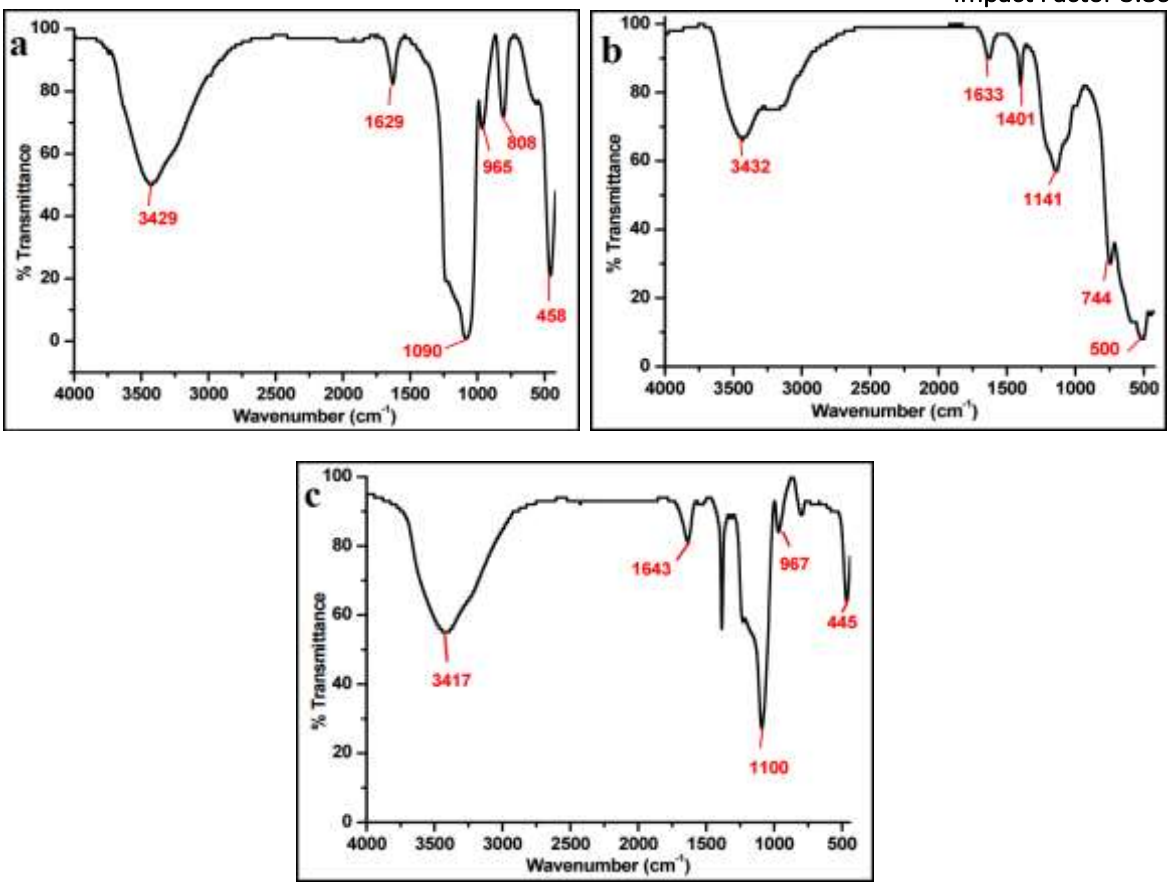

Fig.5: FT-IR spectroscopy: a, b and c for MCM-41, SZ and NiW/SZ-MCM-41catalysts respectively.

Thermal analysis

TGA & DSC of the current catalysts were in the range of 35-550º C. Fig.6(a) for unloaded MCM-41 indicated the weight losses apparently took place at temperatures below 550º C, after which no weight loss could be noticed. The primary weight reduction (4.1%) to 70º C, went with an endothermic peak maximized at 100ºC, seemed to be expected to the elimination of physically adsorbed water. The secondary weight reduction (5.3 %) in the range ~200-350º C indicated that major of the surfactant (CTAB) in the prepared MCM-41 decay. Fig.6(b) for the nano-structured sulfated zirconia showed TGA and DSC where indicated weight losses apparently took place at temperature below 550°C, after which no weight loss could be noticed. The first weight (10.5%) up to 100°C, accompanied with the first exothermic peak at 100°C, seemed to be due to the elimination of physically adsorbed water. The second weight loss (1.64%) in the range 200-350ºC accompanied with the second exothermic peak maximized at 300°C can be attributed to dehydroxylation process. Fig.6(c) for NiW/SZ-MCM-41 catalyst showed TGA and DSC where observed weight losses apparently took place at temperatures below 550º C, after which no weight loss could be noticed. The first weight loss (2%) at less than 100ºC, accompanied with an exothermic peak maximized at 79ºC, seemed to be due to the elimination of physically adsorbed water. The secondary weight reduction (13 %) in the range ~260-300ºC accompanied also with an exothermic peak maximized at 280ºC, indicated beside the loss of physically bound water, the complete decomposition of template of the sample then the sample become stable up to 550°C. In general, the current catalysts have high thermal stability up to 550°C.

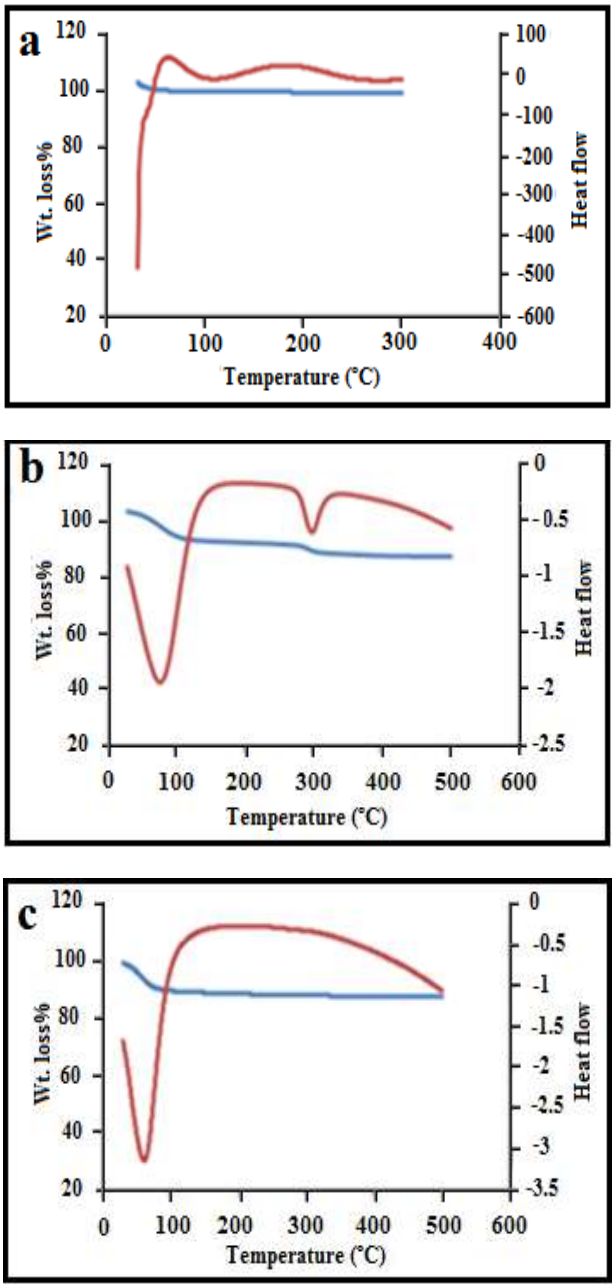

Fig.6: TGA and DSC: a, b and c for MCM-41, nano-structured sulfated zirconia and NiW/SZ-MCM-41 catalyst respectively

Temperature programmed desorption (TPD)

Temperature programmed desorption of adsorbed ammonia was used to measure the acidic intensity of the catalyst. Ammonia adsorbs strongly on the acidic sites in TPD. For sulfated zirconia, Fig. 7(a) indicated that there are weak acid sites at 107°C and super acid sites at 618°C. For NiW/SZ-MCM-41 catalyst, Fig. 7(b) showed that there are weak acid sites at 104°C and very strong acid sites at temperature 473°C. These results showed that NiW/SZ-MCM-41catalyst is suitable to be used in our application.

ISSN 2349-0292
Impact Factor 3.802

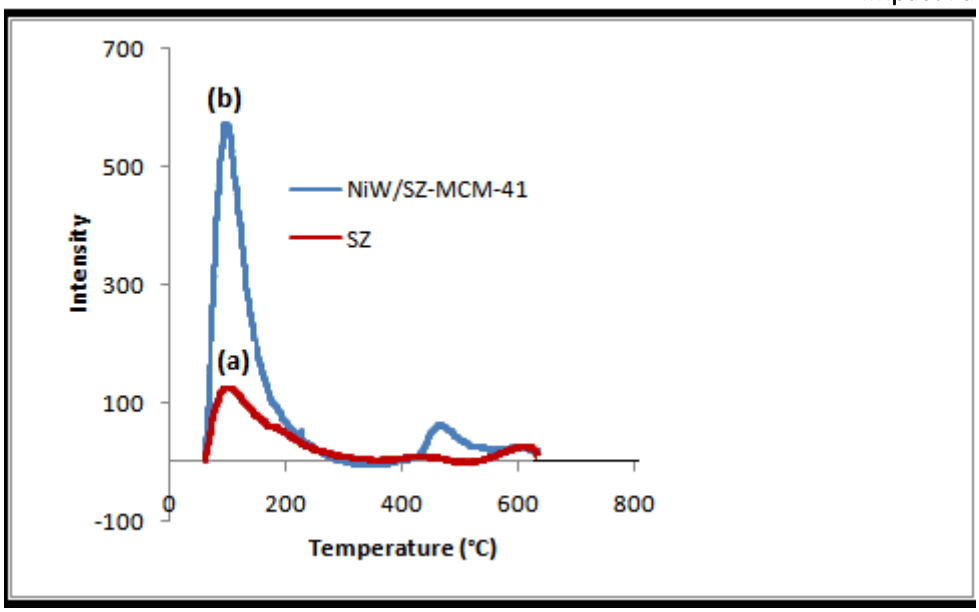

Fig. 7: TPD (a) for Sulfated Zirconia and (b) for NiW/SZ-MCM-41 catalyst

Hydrocracking of oleic acid

Prior to the main study on hydrocracking of oleic acid, a blank test without catalyst was carried out at 425°C, 4MPa for 2hr. The results actually showed a minuscule conversion of oleic acid, however, there was no information of any C_{18} hydrocarbon. The conversion of oleic acid into organic liquid product (OLP) hydrocarbons involve many complex reactions, detailed hydrocarbon composition of all compounds was gotten by means of gas chromatography. This quantitative analysis gave n-paraffins and iso-paraffins ranging between C_5 –C_{18}+. However, the majority of these hydrocarbons include C_5-C_8 hydrocarbons, C_9-C_{14} hydrocarbons and C_{15}-C_{18} hydrocarbons range especially C_9-C_{14} (Fig.8).

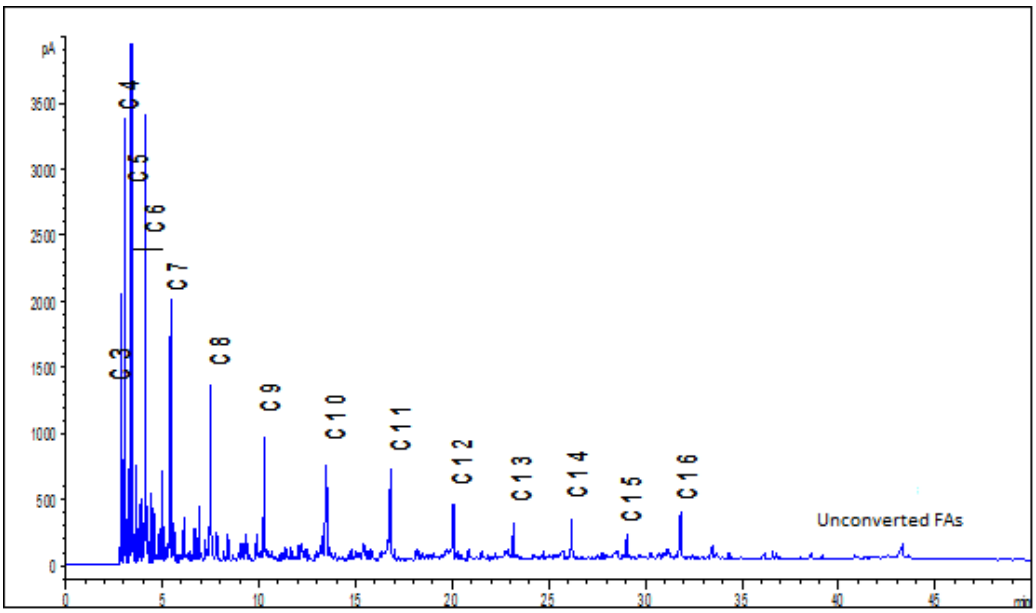

Fig 8: Gas Chromatography of OLP from oleic acid using sulfided NiW/SZ-MCM-41catalyst

ISSN 2349-0292
Impact Factor 3.802

Reaction pathways for conversion of oleic acid into alkanes

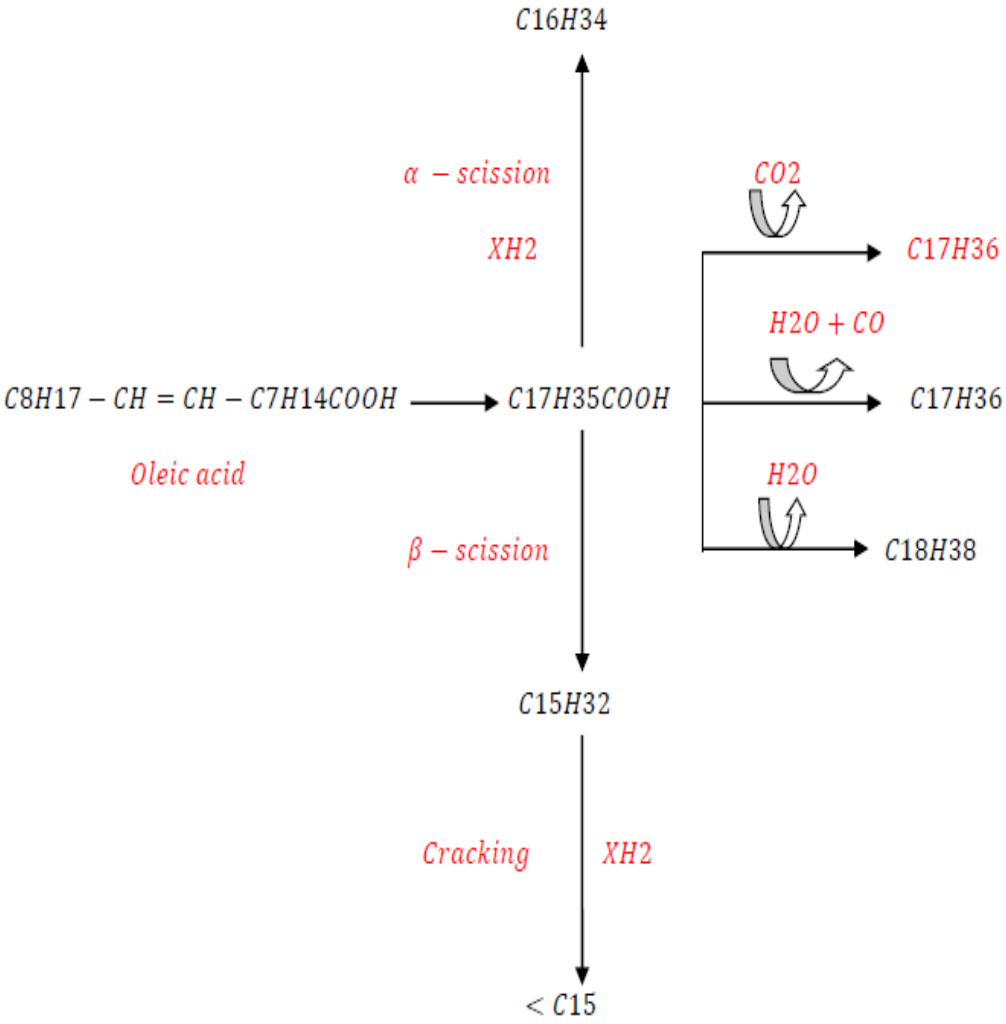

Scheme1. Possible reaction pathway for deoxygenation of oleic acid

Scheme 1 provides possible pathways for deoxygenation of oleic acid (OA), has two functional groups (C=C and COOH) for reaction with hydrogen. Hydrogenation of C=C resulting in stearic acid (SA) happens prior to the deoxygenation reaction. Decarboxylation results in heptadecane (C17) and hydrodeoxygenation yields octadecane (C18). It can be instigated that the $<C_{15}$ hydrocarbons essentially originated from the α/β--C scission reactions [scheme 1].

Table 2 Physical properties of crude OLP at the current conditions

specifications	Crude OLP	Gasoline range(45-160∘C)	Kerosene range (160-275∘C)	Diesel range(275-310 ∘C)	Method
Yield wt.%	88	17	45	27	
Density at 20 ºC, g/cm^3	0.8650	0.7856	0.7904	0.8075	ASTMD-1298
Kinematic viscosity at 40 ºC, cSt	2.55	1.22	2.2	2.4	ASTM D445
Pour point ºC	-39	-36	-36	-24	ASTM D97
Calorific value KJ/Kg	4396	4468	4550	4411	ASTM D240
Sulfur wt.%	Nil	Nil	Nil	Nil	ASTM D 129
Copper stripper corrosion(3h,50ºC)	1a	1a	1a	1a	ASTM D130
Smoke point mm	-	-	23	-	ASTM D1322
Flash pointºC	135	-	68	127	ASTM D92
Aromatics wt. % GC-MS Non-converted FAs Aromatic vol. % Olefins vol. % Paraffins vol. %	 16,64 3.78 	 10.5 2 87.5	 16.28 0.5 83.22	 - - -	 ASTM D1319

Table 2 indicates that the crude OLP (88 wt. % yield) has kinematic viscosity (2.55 CSt), pour point (-39 ºC), calorific value (4396 KJ/Kg) and non-converted free fatty acid (3.78) while the aromatic content 16.64 wt%. The gasoline range distillate (17% yield) contains olefins (2 vol. %) and aromatics (10.5vol.%) which is not good for the burning quality. However, the other properties such as density (0.7856g/cm^3), viscosity (1.22 cSt) and pour point (-36 ºC) seem to be in the suitable of gasoline standers specifications. The kerosene range distillate (45% yield) has acceptable characteristics such as density (0.7904 cm^3), viscosity (2.2 cSt) and pour point (-36 ºC) with a good calorific value (4550KJ/Kg), while the smoke point (23mm) is not very high and the aromatic content (16.28 vol. %). The diesel range distillate (27% yield) showed good density (0.8075cm^3), viscosity (2.4cSt), copper stripper corrosion (1a), pour point (-24ºC), sulfur wt. % (Nil) and calorific value (4411KJ/Kg). The produced kerosene range has good properties if compared with the properties of conventional kerosene. A matter which made it qualified as a source of jet fuel production. Properties of the diesel range distillate obtained were compared favorably with the UOP–Hydro refining green diesel [30].

CONCLUSIONS

NiW/SZ-MCM-41 catalyst was prepared via the wet co-impregnation of nickel nitrate hexahydrate and ammonium metatungstate hydrate then sulfided. Low angle XRD indicated a slight change of intensity of the catalyst to lower 2ɵ values then confirmed by decreasing of BET surface area and pore structure. This indicates the well distribution of metals on the catalyst. The addition of sulfated zirconia, described as super acidic, made this catalyst a strong acidic one. The synthetic catalyst has a high thermal stability that improves the hydrocracking process.

Quantitative gas chromatography detected n-paraffins and isoparaffins ranging between C_5-C_8 (gasoline range), C_9-C_{14} (kerosene range) and C_{15}-C_{18} (diesel range). Distillation of OLP produces get three distillates; gasoline (45-160ºC), kerosene (160-275ºC) and diesel (275-310ºC). The produced kerosene range has good properties comparing with the properties of conventional kerosene which made it qualified as a source of jet fuel production. Properties of the diesel range distillate obtained were favorable with the UOP–Hydro refining green diesel. The sulfided NiW/SZ-MCM-41 catalyst is considered an interesting catalyst for the hydrocracking of fatty acid molecules into gasoline, kerosene and diesel-range hydrocarbons, also, the current operating conditions (temp.= 425ºC, Press.= 4 Mpa, Cat. wt%=5 and time= 2h) were suitable for producing the desired products.

REFERENCES

[1] J.N. Chheda, G.W.Huber, J.A.Dumesic, Liquid-phase catalytic processing of biomass-derived oxygenated hydrocarbons to fuels and chemicals, Angewandte Chemie International Edition, 46 (2007) 7164-7183
[2] Y.C. Lin, G.W. Huber, The critical role of heterogeneous catalysis in lignocellulosic biomass conversion, Energy & Environmental Science, 2 (2009) 68-80
[3] A. Alvarez and J. Ancheyta, Modeling residue hydro processing in a multi-fixed- bed reactor system, Applied Catalysis A: General 351(2008)148-158
[4] S. Bezergianni, A. Kalogianni and I.A. Vasalos, Hydrocracking of vacuum gas oil vegetable oil mixtures for biofuels production, Bio resource Technology 100 (2009) 3036-3042
[5] S. Bezergianni, S. Voutetakis and A. Kalogianni, Catalytic hydrocracking of fresh and used cooking oil, Industrial & Engineering Chemistry Research, 48 (2009) 8402- 8406
[6] M.A. Callejas and M.T. Martínez, Hydroprocessing of a Maya residue. II. Intrinsic kinetics of the asphaltenic heteroatom and metal removal reactions, Energy & fuels, 14(2000) 1309-1313
[7] Isa Y. M.and E. T. Ganda, Bio-oil as a potential source of petroleum range fuels, Renewable and Sustainable Energy Reviews, 81 (2018) 69-75.
[8] B. Donnis, R.G. Egeberg, P. Blom and K.G. Knudsen, Hydroprocessing of bio oils and oxygenates to hydrocarbons, Understanding the reaction routes, Topics in Catalysis, 52 (2009) 229-240
[9] J. Dupont, A.Z.Suarez and M.P. Meneghetti, Catalytic production of biodiesel and diesel-like hydrocarbons from triglycerides, Energy & Environmental Science, 2(2009) 1258-126
[10] N. Taufiqurrahmi and S. Bhatia, Catalytic cracking of edible and non-edible oils for the production of biofuels, Energy & Environmental Science, 2011. 4(4): p. 1087- 1112.
[11] M. Liu, L. S. Yu , B. Xi ,Y. Zhao, X. Xia, MCM-41 impregnated with A zeolite precursor: synthesis, characterization and tetracycline antibiotics removalfrom aqueous solution, Chemical engineering journal, 223 (2013) 678-687
[12] H. Zhu, M. Xue, H. Chen and J.Shen, Dispersion of nano nickel particles over SBA-15 modified by carbon films on pore walls, Catalysis letters, 134 (2010) 93-101
[13] N. Roik and L.Belyakova, Sol–gel synthesis of MCM-41 silica and selective vapor-phase modification of their surface, Journal of Solid State Chemistry, 207 (2013) 194-202
[14] Á. Szegedi, M. Popova, V. Mavrodinova and C. Minchev, Cobalt-containing mesoporous silicas Preparation, characterization and catalytic activity in toluene hydrogenation, Applied Catalysis A: General, 338(2008) 44-51
[15] S. Todorova, V. Pârvulescu, G. Kadinov, K. Tenchev, S. Somacescu and B.L. Su, Metal states in cobalt- and cobalt–vanadium-modified MCM-41 mesoporous silica catalysts and their activity in selective hydrocarbons oxidation, Microporous and Mesoporous Materials, 113(2008) 22-30
[16] A. Corma, From microporous to mesoporous molecular sieve materials and their use in catalysis, Chemical reviews, 97(1997) 2373-2420
[17] T. Okuhara, N.Mizuno, and M.Misono, Catalysis by heteropoly compounds—recent developments, Applied Catalysis A: General, 222(2001) 63-77
[18] S. Biz and M.L. Occelli, Synthesis and characterization of mesostructured materials, Catalysis Reviews, 40(1998) 329-407
[19] A.M. Alsalme, P.V. Wiper, Y.Z. Khimyak, E.F. Kozhevnikova and I.V. Kozhevnikov, Solid acid catalysts based on H 3 PW 12 O 40 heteropoly acid: acid and catalytic properties at a gas–solid interface, Journal of Catalysis, 276(2010) 181-189
[20] Y.Liu, L.Xu, B. Bing, X.Zhi, k. Li, L.Jia and W.Guo, Toluene alkylation with 1-octene over supported heteropoly acids on MCM-41 catalysts, Journal of Molecular Catalysis A: Chemical, 297(2009) 86-92
[21] T.Klimova, L.Pena, L.Lizama, C.Salcedo and O.Y.Gutiérrez, Modification of activity and selectivity of NiMo/SBa-15 HDS catalysts by grafting of different metal oxides on the support surface. Industrial and Engineering Chemistry Research, 48(2009) 1126-1133.
[22] H.I. Meléndez-Ortiz, L.A. García-Cerda,Y. Olivares-Maldonado,G. Castruita, J.A. Mercado-Silva,Y.A. Perera-Mercado, Preparation of spherical MCM-41 molecular sieve at room temperature: Influence of the synthesis conditions in the structural properties, Ceramics international, 38(2012) 6353-6358
[23] J-H. Wang and C.-Y. Mou, Catalytic behavior of nanostructured sulfated zirconia promoted by alumina: Butane isomerization, Catalysis Today, 131(2008) 162-172

ISSN 2349-0292
Impact Factor 3.802

[24] B. AlAlwan, S.O. Salley and K.S. Ng, Biofuels production from hydrothermal decarboxylation of oleic acid and soybean oil over Ni-based transition metal carbides supported on Al-SBA-15, Applied Catalysis A: General, 498 (2015) 32-40
[25] E. Furimsky and F.E. Massoth, Deactivation of hydro processing catalysts,Catalysis Today, 52(1999) 381-495
[26] G.D.Yadav and A.D. Murkute, Preparation of a novel catalyst UDCaT-5: enhancement in activity of acid-treated zirconia—effect of treatment with chlorosulfonic acid vis-à-vis sulfuric acid, Journal of Catalysis, 224(2004) 218-223
[27] A. Sonthalia, N. Kumar, Hydroprocessed vegetable oil as a fuel for transportation sector: A review, Journal of the Energy Institute, 2017 https://doi.org/10.1016/j.joei.2017.10.008
[28] A. Sinhamahapatra, N.Sutradhar, M.Ghosh, H.C.Bajaj and A.B.Panda, Mesoporous sulfated zirconia mediated acetalization reactions, Applied Catalysis A: General, 402(2011) 87-93
[29] B.Rakshe, V. Ramaswamy, S.G. Hegde, R.Vetrivel and A.V. Ramaswamy, Crystalline, microporous zirconium silicates with MFI structure, Catalysis letters, 45 (1997) 41-50
[30] T. N. Kalnes, T. Marker, D.R. Shonnard and K.P. Koers, Green diesel production by hydro-refining renewable feed-stocks, www.biofuels-tech.com (2008) 7- 11